

# A High-Performance Sailplane Airfoil with Variable Upper-Surface Contour

Götz Bramesfeld  
*The Pennsylvania State University*  
*University Park, PA 16801, USA*  
*pipa@psu.edu*

Peter Wierach  
*German Aerospace Center (DLR)*  
*38108 Braunschweig, German*  
*Peter.Wierach@dlr.de*

Christian Ückert and Reiner Kickert  
*Flugtechnik & Leichtbau*  
*38108 Braunschweig, Germany*  
*yeti@eta-aircraft.de*

This paper was presented at the 15<sup>th</sup> International Conference on Adaptive Structures and Technologies in Bar Harbor, ME, Oct. 25-27, 2004. It is reprinted with permission.

## Abstract

In a feasibility study, an airfoil was developed that satisfies the complex requirements of high-performance sailplanes with a variable upper-surface contour. The base wing, which includes the non-deformable lower surface, an internal torsion box, as well as a spar, is designed to carry the loads and moments typical of a 15-meter span Racing-Class sailplane. The flexible skin of the upper-surface is attached to the leading edge of the base airfoil and to four linkage points of a mechanical drive. The chordwise stiffness distribution of the composite skin is tailored so that the two desired contours are accomplished in conjunction with the mechanical drive. The thin version has a maximum thickness of 11.8% chord, while the thick airfoil 14.4% chord. A cruise flap allows a further adjustment of the airfoil performance to different flight speeds. The performance estimation for a Racing-Class sailplane with the new airfoil shows significant increases in average cross-country speeds that are, depending on the weather model, up to 5% faster than using conventional airfoils.

## Introduction

One of the major aspects of competition soaring is to fly a given course with the fastest possible average cross-country speed. Speeds of over 100km/h for a course of 300 km and more are commonly flown with modern high-performance sailplanes. The average speed is the result of the sailplane going through a cruise-climb cycle, in which it cruises at elevated speeds and, then, regains the lost altitude by circling in thermals. Consequently, the average cross-country speed is maximized by reducing the time spent climbing and by increasing the cruise part of the cross-country flight. The optimum speed during cruise depends on the average strength of the climb rates that can be realized while thermalling [1]. In general, the higher the climb rate of the glider, the faster the optimum cruise speed is and, consequently, the faster is the average cross-country speed.

Although the climb performance depends on the strength and size of the thermals, it also depends on the ability of the glider to efficiently exploit the rising air of a thermal. This often requires tight circling in order to stay in the core of the thermal as a traded-off against maintaining a low sink rate of the glider in order to achieve the best net climb. A very

simplified conclusion is that, in order to maximize climb performance, a glider needs a wing with either a large area or one that produces high lift coefficients.<sup>1</sup>

The cruise performance is often measured with the lift-to-drag ratio or glide ratio, which indicates the distance that a sailplane can glide from a given altitude in calm air. Modern Racing-Class sailplanes have maximum lift-to-drag ratios up to about 50. A reduction in the aircraft drag increases the lift-to-drag ratio. During cruise, approximately half of the total drag is due to the profile drag of the wing [1], which depends on the total wing area and the section drag. Thus, the cruise performance is improved either by reducing the total wing area or the section-drag of the wing. The latter approach has led to the extensive usage of laminar airfoils in soaring over the past 50 years.

The conflicting requirements on the wing for cruise and climb make the design of a sailplane wing an extremely

---

<sup>1</sup> Indeed, the ratio  $C_L^{1.5}/C_D$  needs to be maximized in order to minimize the sink rate of the glider.  $C_D$  is the overall drag coefficient and  $C_L$  the lift coefficient.

challenging task that requires the consideration of a multitude of weather models and piloting tasks [2-4]. A wing optimized for cruise does not necessarily provide the high-lift properties that are needed for thermalling and vice versa. Furthermore, wings that are designed for low cruise drags often have undesirable handling qualities at the low speeds of thermalling.

Several attempts have been made to accommodate the conflicting flight regimes with variable-wing geometries. The most commonly used solution is the trailing edge flap. Within limits, it allows an adjustment of the airfoil performance, in particular the low-drag region, to the given requirements. The flap is relatively simple in structure and has low activation loads. Other approaches of variable-wing geometries are, for example, the sailplanes FS-29 and SB 11, shown in Figs. 1 and 2. The FS-29, which flew first in 1975, has a telescoping wing to achieve variable span. In flight, the pilot can vary the wingspan between 13 and 19 meters. The SB-11, which first flew in 1977, has a variable wing chord that allows the pilot to increase the wing area by 33 percent. Despite the clear performance advantages of the telescoping-wing and variable-chord concepts, the additional mechanisms and structure required cause them to be less suitable for the general soaring community due to the increase in weight and complexity.

A new concept was explored in a feasibility study of an airfoil with a variable upper-surface contour that can be adapted to the different requirements of the high and low speed-flight regimes typical for soaring [5-7]. The objective is to maximize the gains in drag reduction through increased laminar flow lengths on the upper surface without having to pay a penalty at low speeds. Modern low-drag, laminar airfoils of high-performance sailplanes have laminar flow over most of their lower surface, some up to 95% chord. Thus, very little gain in drag reduction appears to be possible there. On the upper surface, however, the maximum length of laminar flow is much more limited to about 60% chord. The relative early transition is needed in order to provide sufficient chord length to safely recover the pressure from its leading-edge suction-peak at high angles of attack. Otherwise, if the adverse pressure gradient is too steep, the flow will separate with a subsequent deterioration of the flight properties in the high-lift regime.

The concept explored in this study uses two distinct upper-surface contours. The one designed for cruise at low lift coefficients has low drag due to extended laminar flow along the upper and lower surfaces. The second contour supports a pressure recovery without flow separation, despite high leading-edge suction peaks at maximum lift. The feasibility study explored the practicality of such an airfoil and the possible performance gains for a sailplane. For the case study, sizing and loads are representative to the ones that are typical of the center-wing section of a modern Racing-Class sailplane.

### **Airfoil-Design Objectives and Constraints**

The basic concept of the airfoil with a variable upper-surface contour is shown in Fig. 3. The base wing, which

includes the non-deformable lower surface, an internal torsion box, as well as a spar, is designed to carry the loads and moments typical for a 15-meter span, Racing-Class sailplane. The flexible upper-surface skin is made from composite material and attached to the base wing at the leading edge and at four linkage points of the drive mechanism. The trailing edge of the flexible skin is free to slide on the aft part of the base wing in order to compensate for the change in arc length when moving between the two upper-surface contours. The number of contour variations is limited to two different shapes, a thin and a thick version. Additionally, a conventional trailing edge flap allows further adjustment of the airfoil performance to the different flight regimes.

### **Aerodynamic requirements**

An example of a drag polar of a laminar airfoil is plotted in Fig. 4. In general for sailplanes, the airfoil operates during cruise at the lower lift coefficients within the low drag range near Point A. Thermalling is usually done around the upper corner, or Point B. The maximum section-lift coefficient at Point C influences the minimum or landing speed of the aircraft and, consequently, the wing size. Point A depicts the lower edge of the low-drag region, where as Point B marks the upper edge. Within the low-drag region, the transition points from laminar to turbulent flow remain relatively stationary on the upper and lower surfaces. Beyond the boundaries of the low drag region, adverse pressure gradients cause the transition points to move forward and drag increases due to more turbulent flow. The transition point of the lower surface remains relatively fixed until it moves forward rapidly at lift coefficients below Point A, whereas the upper-surface transition-point moves forward at lift coefficients above B. In addition to higher skin-friction drag, the increasing amount of turbulent flow leads to greater tendency of turbulent flow separation that starts at the trailing edge and spreads upstream with increasing angles of attack. The rapidity of the forward motion of the upper-surface transition from Point B to C can be tailored and has significant influence on the low-speed handling qualities of the sailplane [5].

In this study, an essential requirement on the thick version of the airfoil with a variable upper surface is that it produces a maximum lift coefficient similar to those of the HQ-17 and CA2 airfoils that were used as slow-speed benchmarks. Above the low-drag region and up to the maximum lift coefficient, the lift curve is desired to behave similarly to the ones of the benchmark airfoils. Generally, the comparison airfoils are associated with very agreeable low-speed handling qualities [5].

In its cruise configuration, the thin version desirably has a low-drag range of similar width and over a similar lift-coefficient range as the airfoils, HQ-17 and CA2. The minimum drag coefficient, however, is to be comparable to that of the HQ-35. This particular airfoil has one of the lowest drag coefficients of any wing airfoil used on sailplanes. Its slow-speed handling qualities, however, are less favorable.

Besides the two different upper-surface shapes, the airfoil is equipped with a trailing edge flap. To limit the pilot-work load, the number of flap settings is restricted to two for the thick airfoil version and to three for the thin one. The two flap settings of the thick version are meant for thermalling, with the most positive also used for landing. The three flap settings of the thin version are supposed to allow limited thermalling and slow cruise, as well as intermediate fast and fast cruise. The different flap settings overlap sufficiently in airspeed in order to reduce the performance loss due to any possible piloting error.

A further requirement is that the airfoil performance is relatively insensitive to surface imperfections. This requirement is to limit the influence of manufacturing imperfections or secondary deformations of the flexible upper surface due to the loads of the pressure distribution. Stall and low-speed behavior are desirably independent of any contamination of the wing, for example due to bugs or water.

### Structural requirements

The structural design requirements of the load-carrying base wing are driven by the loads that are representative for the wing-root section of a Racing-Class sailplane with 15-meter span, as indicated by the shaded area in Fig. 5. In general, the shear forces and bending moment due to lift are largest there. The latter value determines the minimum required height of the spar, which consequently defines the minimum allowable thickness of the thin configuration of the variable airfoil.

The flexible upper-surface skin has to be sufficiently flexible in chordwise direction so that it can be shaped to the desired contour. In spanwise direction, however, the flexible skin has to be adequately stiff between the locations of the drive mechanism in order to limit its deformation under the influence of the airloads. Beyond that, any waviness in chordwise direction has to be kept small in order not to cause premature transition to turbulent flow.

### Drive mechanism requirements

The drive mechanism has to be able to change the flexible skin and support the deformed upper surface so that the desired contours are maintained despite large airloads. In order to stay within the rules for racing sailplanes, the change of contours has to be possible manually, without any additional boost power. Figure 6 shows the different loads that act on a deformable upper surface. The upper surface produces roughly two-thirds of the lift required, which is approximately 3 kN during steady, level flight. The loads are even higher with elevated load factors due to gusts or banked angle. If the relaxed upper surface skin is the thin contour, the loads due to the elastic deformation will act against the airloads. The remaining work that the pilot has to exert in order to change between the surface contours during flight is limited by human strength and the space available in the cockpit. Most preferable is a simple hand lever with a maximum travel of about 50 cm and reasonable activation

forces. Systems that require pumping have been less feasible in soaring [7].

The space available for the drive mechanism is limited and mainly restricted between the load carrying base wing and the flexible upper-surface skin. In the thin configuration, the aerodynamic and structural requirements leave roughly 15 mm of space for the mechanism. Between the locations of the drive mechanisms that are spaced 90 cm in the spanwise direction, the desired shapes are ensured with spanwise stiffeners. These also have to fit in the space between the base wing and the flexible upper surface of the thin version.

A further requirement is that the mechanism be relatively simple and have a limited number of linkage points. This simplifies the design process and reduces the part count, which means a smaller manufacturing and maintenance effort, as well as less additional weight. An uncomplicated drive system also reduces the chances of failure.

### The ALDI-9 Design

The Aldi-9 airfoil in its thin and thick configuration is shown in Fig. 7. Also depicted in this figure are the internal structure and the drive mechanism with which the upper-surface contour is deformed. The name is the German abbreviation of *adaptive Laminarprofil variable Dicke*, which translates to adaptive laminar airfoil with variable thickness. It is the ninth aerodynamic design. The maximum thickness of the thin version is 11.8% with respect to the chord length and 14.4% for the thick configuration. The location of the maximum thickness moves forward from 43.5% chord to 40.8% chord when changing from thin to thick. The trailing edge flap is 13.5% of the total chord.

### The base wing structure and upper-surface skin

The load-carrying base wing of the adaptable airfoil, Aldi-9, has a relatively conventional composite structure typical for modern sailplanes. The structural designs of the base wing and trailing-edge flap are in accordance with [8]. A carbon-fiber composite skin of the base wing provides the needed torsional stiffness. The constraint in spar height of 70 mm or 7.8% of the chord necessitates a double box spar for sufficient strength for the bending moment that results from the spanwise lift distribution. Besides reacting to the shear force due to lift, the four spar webs increase the buckling stiffness of the relatively thin spar caps that are made from carbon fiber.

Initially, the deformation of the flexible skin was optimized using a 2-D FEM-beam model, in which the thickness of the beam elements is varied in chordwise direction in order to get the desired stiffness distribution. As shown in Fig. 8, the desired bending line of the upper-surface skin is achieved with a fiberglass-composite lay-up that has a varying thickness in chordwise direction. The predominant fiber orientation is  $0/90^\circ$ . Once the appropriate lay-up had been found, a 3-D FEM model of the flexible skin with a span of 0.9 m was used to determine the deformations between the mechanical actuators due to the superimposed aerodynamic

loads. The grid of the model is shown in Fig. 9. Four spanwise stiffeners serve as attachment points for the mechanical-drive system and increase the stiffness between them. As shown in Fig. 10, the deviations from the desired contour increase with distance from the actuator locations. Nevertheless, they remain within the design limits. The deformed contours were reanalyzed for their aerodynamic quality. The 3-D FEM model also provided the loads for determining the actuator loads. A more thorough description of the structural design of the base wing and of the trailing-edge flap, as well as the design and the analysis of the flexible skin is in [6].

### Drive mechanism design

A sketch of the drive mechanism that deforms the upper surface skin is shown in Fig. 11. The mechanism is discussed more detailed in [7]. In principal, it consists of five links that connect through four sliders. The deformable skin is attached to the drive at four points. As can be seen in Fig. 7, a bell crank located between the two spars is the main drive that moves the linkages. The bell crank is activated by a system of pushrods, of which the main drive is located along the leading edge of the wing and connects to the controls in the fuselage. Also shown in Fig. 11 is a system of comb-like ribs that help shape the different leading-edge radii of the two thickness versions of the airfoil.

The estimated loads to activate the mechanism in flight are suitable for easy handling by the pilot [7]. The loads are the result of the pressure distribution, the elastic deformation of the flexible skin, and a spring that pulls the flexible skin tight at its trailing edge.

### Airfoil characteristics and performance

The predicted aerodynamic characteristics of the thin Aldi-9 with its cruise-flap setting are plotted in Fig. 12. Also shown in this figure are the values for the HQ-35 and the CA2 in their cruise settings. In order to account for the dependency between speed and lift coefficient during steady flight and for a given wing area and gross weight, the chord-Reynolds number is adjusted so that  $Re\sqrt{c_1} = 105100$ . The Aldi-9 has a similarly wide low-drag region as the benchmark-cruise airfoils, HQ-35 and CA2. The theoretical drag values of the Aldi-9 are slightly lower than the ones of the HQ-35 and significantly lower than the ones of the CA2.

The performance of the thick Aldi-9 version with its high-lift flap setting is shown in Fig. 13. Its drag and lift curves are very similar in values and shapes to the ones of the comparison airfoils of the high-lift regime, HQ-17 and CA2. The relatively small differences in drag are of little significance in this flight regime, where the induced drag of the wing dominates. Again,  $Re\sqrt{c_1} = 105100$  was kept constant.

A sample pressure distribution of the thin Aldi-9 version is shown in Fig. 14. Laminar flow is maintained past 85% chord on the lower surface. Transition is forced with a turbulator at 76% chord on the upper surface. In the

feasibility study discussed here, such pressure distributions were imposed onto the FEM model in order to determine the secondary elastic deformations of the flexible surface due to the airloads [6]. They were also used to estimate the activation loads required to change between the two thickness versions [6,7]. The contours that were generated with the FEM model with superimposed external loads were re-analyzed with XFOIL for their aerodynamic performance. It was found that the degradation in performance due to the secondary elastic deformations is limited [5]. A more complete discussion of the aerodynamic design is listed in [5].

The performances of a Racing-Class sailplane with the different wing airfoils, Aldi-9, HQ-35, HQ-17, and CA2, were computed in order to assess the gains due to the Aldi-9 [5]. The configuration of the theoretical Racing-Class sailplane employed is the one that formed the basis of the structural design. With the exception of a 10% higher wing weight due to the additional structure and mechanism required in the case of the adaptive airfoil, no further configuration changes were made. An example of the resulting glide-ratio and speed polars is plotted in Fig. 15 for the sailplane using the Aldi-9 airfoil. These performance estimates were used to predict the average cross-country speeds based on a theoretical weather model [1,5]. The results are summarized in Table 1. Although the Aldi-9 has only a slight advantage over the HQ-35 in maximum glide performance, its superior thermalling performance results in a nearly 5% higher average cross-country speed. This is significantly faster, when considering that during soaring contests one or two percentage points often separate the winner from the middle field. The advantages over the other airfoils are similarly large [5].

### Conclusions

The study discussed here demonstrates the general feasibility of an airfoil with a variable upper-surface contour in order to increase the performance of a modern sailplane. Significantly faster average cross-country speeds are predicted for a theoretical Racing-Class sailplane that uses such an adaptable airfoil. The change between the two upper-surface contours is accomplished with a manually activated mechanical drive and a flexible composite skin that has a tailored chordwise stiffness distribution.

The technical realization of such adaptive airfoil is possible, however, further refinements are needed for the aerodynamic design and the performance estimate in order to better judge its full potential. The aerodynamic design neither reaches the potential limits of laminar flow on the upper surface of the thin version, nor fully explores the possibilities of modifying the high-lift range of the airfoil in combination with the wing geometry. Clearly, the design of the airfoil and the wing are interdependent. The accuracy of the performance prediction can be further improved, for example with a better weight estimate.

## References

1. Thomas, F., *Fundamentals of Sailplane Design*, College Park Press, MD, 1999.
2. Horstmann, K., "Evolution of Airfoils for Sailplanes," AIAA-2003-2779, AIAA International Air and Space Symposium and Exposition: The Next 100 Years, Dayton, Ohio, July 14-17, 2003.
3. Maughmer, M.D., "The Evolution of Sailplane Wing Design," AIAA-23003-2777, AIAA International Air and Space Symposium and Exposition: The Next 100 Years, Dayton, Ohio, July 14-17, 2003.
4. Kensch, C., "The Influence of Materials on the Development of Sailplane Design," AIAA-2003-2778, AIAA International Air and Space Symposium and Exposition: The Next 100 Years, Dayton, Ohio, July 14-17, 2003.
5. Bramesfeld, G., "Aerodynamische Auslegung eines Profils mit adaptiver Vestellung der Oberseitenkontur," Studienarbeit, Institut für Leichtbau, Technische Universität Braunschweig, Germany, May 1997.
6. Wierach, P., "Konstruktion und Dimensionierung der Primärstruktur eines Windkanalmodells für ein Profil mit adaptiv veränderbarer Oberseitenkontur," Studienarbeit, Institut für Leichtbau, Technische Universität Braunschweig, Germany, May 1997.
7. Ückert, C., "Detailkonstruktion des Verstellmechanismus für ein Windkanalmodell mit adaptiver veränderbarer Oberseitenkontur," Studienarbeit, Institut für Leichtbau, Technische Universität Braunschweig, Germany, May 1997.
8. "JAR-22: Sailplanes and Powered Sailplanes," Joint Aviation Authorities, Hoofddorp, The Netherlands, 1989.

(Table and Figures on following pages)

Table 1  
 Predicted performances of the given Racing-Class  
 sailplane using different airfoils.

Airfoil	$L/D_{max}$	$V_{L/Dmax}$ [km/h]	Average Cross-Country Speed [km/h]
HQ-35	48.4	107.6	100.6
HQ-17	45.5	105.3	99.5
CA2	46.7	105.9	101.0
Aldi-9	49	106.4	104.9

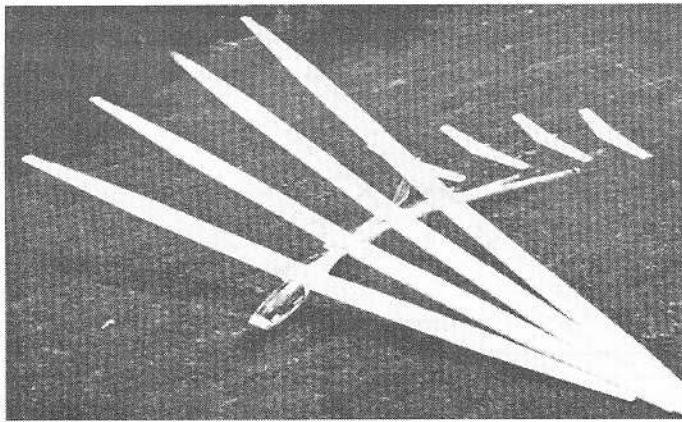


Figure 1 The FS-29 with its telescoping wing (Akaflieg Stuttgart, 1975).

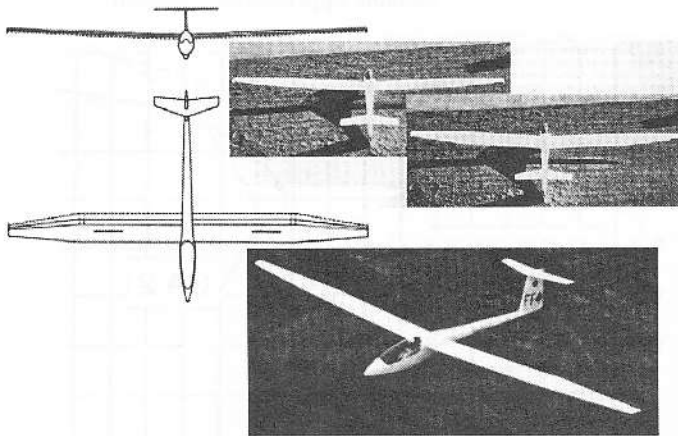


Figure 2 The SB-11 with its fowler flap (Akaflieg Braunschweig, 1977).

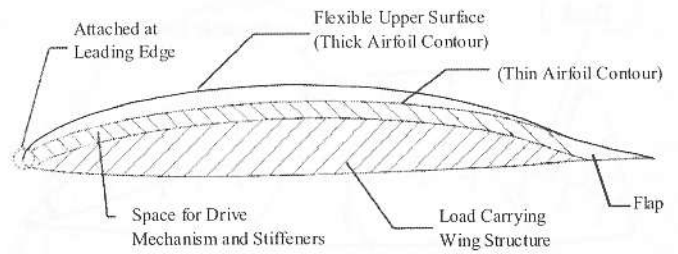


Figure 3 The concept of an airfoil with a variable upper-surface contour.

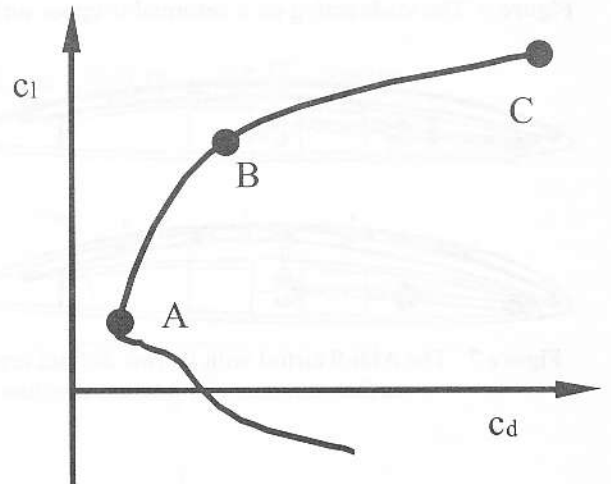


Figure 4 Typical drag polar of a laminar airfoil. The letters are defined in the text.

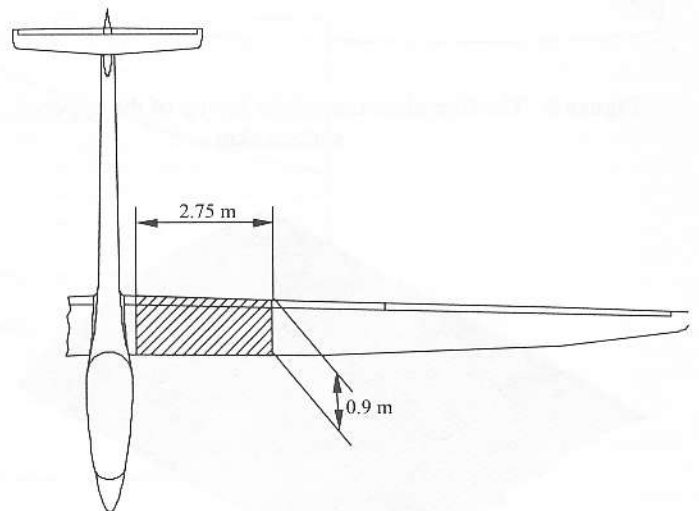


Figure 5 The shaded wing section of the theoretical Racing-Class sailplane is the bases for the structural design.

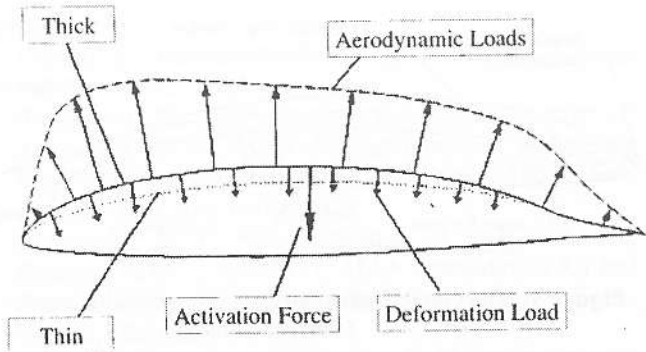


Figure 6 The loads acting on a deformable upper surface.

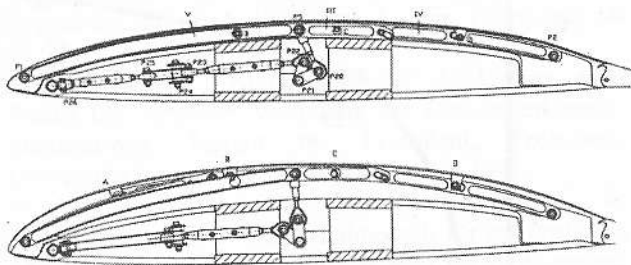


Figure 7 The Aldi-9 airfoil with its two distinct upper-surface contours and internal structure.

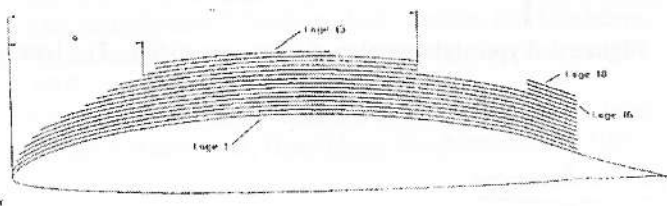


Figure 8 The fiberglass-composite lay-up of the upper-surface skin.

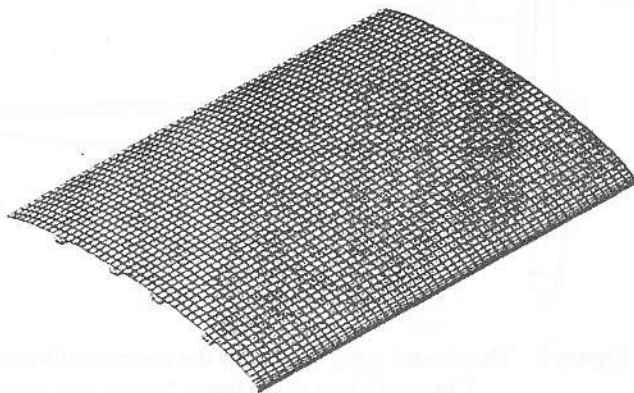


Figure 9 The FEM grid of the upper-surface skin.

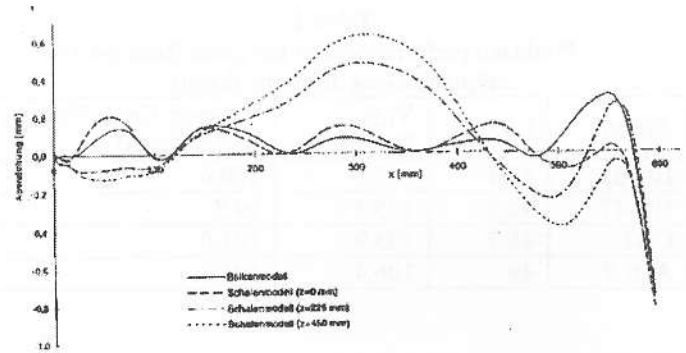


Figure 10 The deformations of the skin at different spanwise locations of the 3-D FEM model due to the aerodynamic loads.

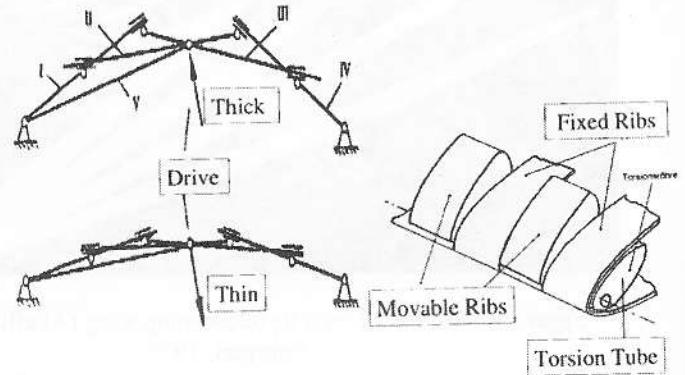


Figure 11 Schematics of the drive mechanism for the variable upper-surface contour.

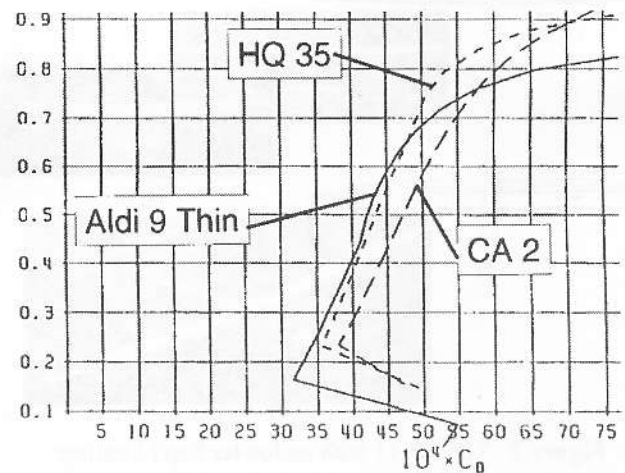


Figure 12 Drag polars of HQ-35, CA2, and Aldi-9 Thin.  
 $Re\sqrt{c_1} = 105100$ .

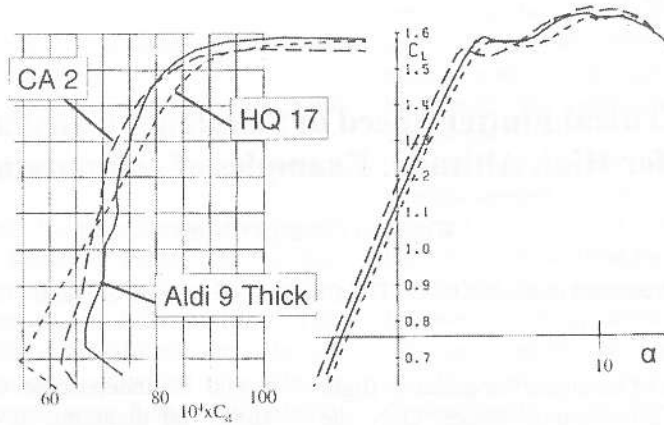


Figure 13 Drag polars and lift curves of HQ-17, CA2, and Aldi-9 Thick.  $Re\sqrt{c_1} = 105100$ .

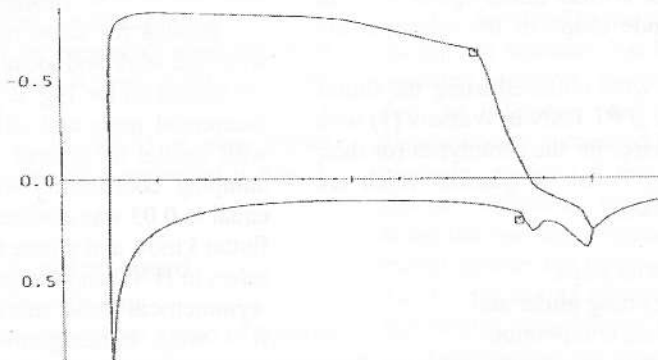


Figure 14 A typical pressure distribution of the thin Aldi-9 at a cruise angle of attack.

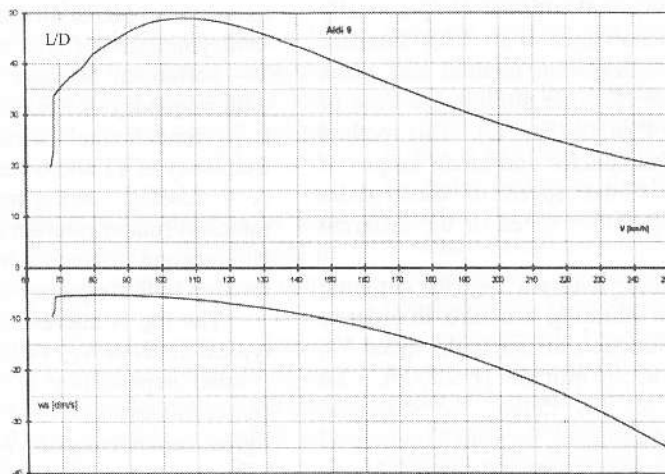


Figure 15 Predicted glide-ratio and speed polar of the given Racing-Class sailplane using the Aldi-9.